

# SIMULATION OF *CERES* AND *GERB* TOA PRODUCTS OVER THE VALENCIA ANCHOR STATION FOR *GERB* VALIDATION PURPOSES

A. Velázquez Blázquez<sup>1</sup>, A. Cano<sup>1</sup>, N. Clerbaux<sup>2</sup>, S. Dewitte<sup>2</sup>, C. Doménech<sup>1</sup>, V. Estellés<sup>3</sup>, A.G. Ferreira<sup>1</sup>, L. González Sotelino<sup>2</sup>, J. Jorge Sanchez<sup>4</sup>, N.G. Loeb<sup>5,6</sup>, D. Pino<sup>4,7</sup>, A. Rius<sup>7</sup>, G. L. Smith<sup>5,8</sup>, Z. P. Szewczyk<sup>5,9</sup>, R. Tarruella<sup>4</sup>, J. Torrobella<sup>7</sup>, S. Vidal<sup>1</sup>, E. Lopez-Baeza<sup>1</sup>

(1) Climatology from Satellites Group, Dept. of Physics of the Earth and Thermodynamics, University of Valencia, Spain

(2) Royal Meteorological Institute of Belgium (RMIB), Belgium

(3) Solar Radiation Group, Dept. of Physics of the Earth and Thermodynamics, University of Valencia, Spain

(4) Polytechnic University of Catalonia, Spain

(5) NASA Langley Research Centre (LaRC), VA, USA

(6) Hampton University, VA, USA

(7) Institute of Space Studies of Catalonia, Spain

(8) National Institute for Aerospace, Hampton, VA, USA

(9) Science Systems and Applications Inc, Hampton, VA, USA

## Abstract

The *Geostationary Earth Radiation Budget (GERB)* instrument on board *Meteosat-8* and *-9* provides accurate measurements of shortwave and longwave broadband radiances and fluxes at the Top of the Atmosphere (TOA) with very high temporal resolution of 15 minutes.

The aim of the study presented here is to validate radiances and fluxes at the TOA measured by *GERB* during the *IV GERB Ground Validation Campaign* at the *Valencia Anchor Station (VAS)* area (31<sup>st</sup> July – 6<sup>th</sup> August 2006). In the study, *GERB* enhanced spatial resolution data (*GERB High Resolution*) is used, where the resolution of the computed fluxes is improved through the combination of well-calibrated *GERB* broadband data with SEVIRI narrow-band high-sampling-rate data. The resolution enhancement process transforms accurate fluxes computed at *GERB* footprint original resolution (nominally 50 km x 50 km at nadir) to a 3\*3 SEVIRI footprint resolution (nominally 9 km x 9 km at nadir). *Clouds and the Earth's Radiant Energy System (CERES)* Terra FM2 data is also used from dedicated PAPS (*Programmable Azimuth Plane Scanning*) observations over the study area during the campaign.

The validation capabilities of the Valencia Anchor Station have previously been assessed by successfully reproducing *CERES* TOA radiances and fluxes with the occasion of different ground validation campaigns. The methodology consists in performing radiative transfer simulations of *CERES* and *GERB* TOA radiances and fluxes from independent ground measurements of surface and atmospheric parameters (such as derived precipitable water vapour content from CIMEL sunphotometer and GPS (*Global Positioning System*) instruments, radiosoundings from the Spanish stations of Madrid and Murcia, aerosol optical thickness also from CIMEL, broadband albedo and temperature over shrubs, bare soil and vineyards in the study area) in conjunction with other satellite products such as TOMS (*Total Ozone Mapping Spectrometer*) ozone, *CERES/SARB* emissivity and MODIS BRDF (*Bidirectional Reflectance Distribution Function*). The latter allows us to analyze the contribution of each land use to the anisotropy of the shortwave radiation field and constitutes a good improvement of the methodology that had been tested for the case of *CERES* in previous campaigns. The comparison between simulations and *CERES* calibrated and validated data provides a good indicator of the reliability of the methodology to be applied as a validation tool for *GERB*.

The results presented here show the comparison between simulated and measured *CERES* and *GERB* radiances under clear sky conditions for the campaign dates.

## 1. METHODOLOGY

This work aims to validate *GERB* high resolution radiances and fluxes at the TOA during the *IV GERB Ground Validation Campaign*, carried out at the Valencia Anchor Station (VAS) between the 31<sup>st</sup> of July and 6<sup>th</sup> of August 2006. In order to achieve this objective the methodology has first been tested and assessed for *CERES* PAPS specifically programmed observations over the study area during the *II GERB Ground Validation Campaign* held in the same area between the 9<sup>th</sup> and 12<sup>th</sup> of February 2004.

The methodology consists in performing a number of radiative transfer simulations for both *CERES* and *GERB* instruments corresponding measured TOA radiances and derived fluxes for the campaign dates. STREAMER (Key et al, 1998) radiative transfer code has been used to perform the simulations, in which radiances and fluxes are computed using the discrete ordinate solver, DISORT version 2 (Stamnes et al, 2000).

Surface and atmospheric parameters used in the radiative transfer simulations were gathered in the campaigns.

### 1.1 Description of field campaigns data

#### *II GERB Ground Validation Campaign*

During this campaign two in-situ radiosounding ascents per day were launched during *CERES* FM2 and FM3 overpasses over the study area; precipitable water vapour content was obtained from simultaneous GPS measurements; atmospheric transmissivity from EKO sunphotometer measurements and broadband albedo and surface temperature were measured at the VAS and in a mobile station placed on a low-vegetation trees and shrubs area.

#### *IV GERB Ground Validation Campaign*

In this campaign precipitable water vapour content was not only obtained from GPS measurements but also from CIMEL sunphotometer retrievals. For this campaign radiosounding ascents from the Spanish Institute for Meteorology stations of Madrid and Murcia were used, aerosol optical thickness was measured with a CIMEL instrument, and broadband albedo and temperature were measured over shrubs, bare soil and vineyards in the study area.

In both campaigns total column amounts of ozone were obtained from TOMS (*Total Ozone Mapping Spectrometer*) values, emissivity from *CERES*/SARB and BRDF (*Bidirectional Reflectance Distribution Function*) of the surface was derived from MODIS BRDF data for every *CERES* and *GERB* footprint using the convolution through each instrument PSF (Point Spread Function). This will allow us to analyze the contribution of each land use to the anisotropy of the shortwave radiation field and constitutes a good improvement of the methodology that had been tested for the case of *CERES* in previous campaigns.

### 1.2 Selection of atmospheric profiles

Temperature and pressure profiles are obtained from the radiosounding ascents. Water vapour is also obtained from the radiosounding ascents but it is interpolated to 1m resolution and completed either with standard MLW (Mid Latitude Winter) or MLS (Mid Latitude Summer) profiles, depending on the campaign period; around 94-95 levels are selected for the simulations. The total column amount of water vapour is scaled to the amount retrieved with the GPS. In this way, we take advantage of the better temporal resolution of the GPS data but also keeping the water vapour profile in the troposphere. (Figures 1 and 2)

As far as the aerosol profile is concerned, we use the STREAMER MLW or MLS (Mid Latitude Winter or Summer) standard atmosphere profile, assuming background tropospheric aerosols and background stratospheric aerosols, with the aerosol optical thickness obtained from the on-ground transmissivity measurements in the case of the February Campaign and from on-ground CIMEL CE-318 retrievals on the August 2006 campaign (Figure 3).

Ozone profile corresponds to the STREAMER Mid Latitude Winter or Summer profiles scaled to the TOMS (*Total Ozone Mapping Spectrometer*) measurements (<http://toms.gsfc.nasa.gov>)

### 1.3 Selection of surface parameters

Surface temperatures were measured at the VAS and at the mobile station, weighting the contribution of each one in the whole area by taking into account the land use classification of the study area (Figure 4).

Surface emissivity (Wilber et al, 1999) is obtained from CERES/SARB (Surface and Atmospheric Radiation Budget) database (<http://www-surf.larc.nasa.gov/surf/>)

To simulate the anisotropy of the radiances at the TOA, it is assumed that radiances at the TOA are sensitive to the anisotropy of surface reflectance and its evolution along the day. This fact makes the BRDF a key parameter to be used in validation studies. In this study, bidirectional reflectance of the surface is calculated from the isometric, volumetric and geometric Kernels (Figure 5) of the MOD43B1 product for the Ross-Thick-Li-Sparse-Reciprocal model (Wanner et al, 1995) in this way:

$$BRDF = k_0 + k_1 \cdot f_{ross-thick} + k_2 \cdot f_{li-sparse}$$

Taking into account that the parameters maintain a linear relation with the bidirectional reflectance, it is possible then to pass from a homogeneous surface to a heterogeneous one composed of homogeneous surfaces, i.e, we will be able to pass from 1km resolution BRDF's to the needed resolution to simulate either CERES or GERB behaviour.

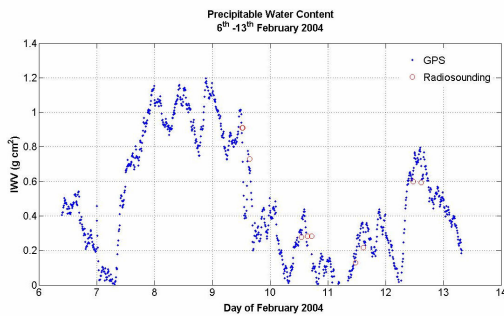


Figure 1: Comparison between precipitable water content measurements from the GPS receiver (blue dots) and radiosounding ascents (red circles)

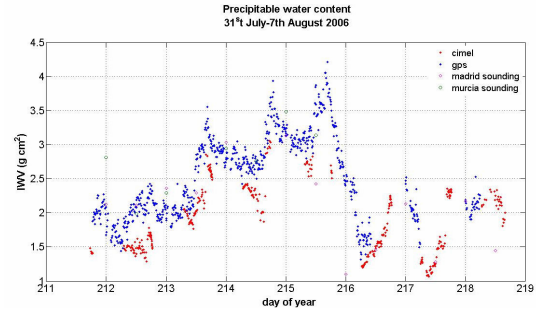


Figure 2: Comparison between precipitable water content measurements from the GPS receiver (blue dots), CIMEL estimations (red dots), radiosounding ascents (pink squares and green squares)

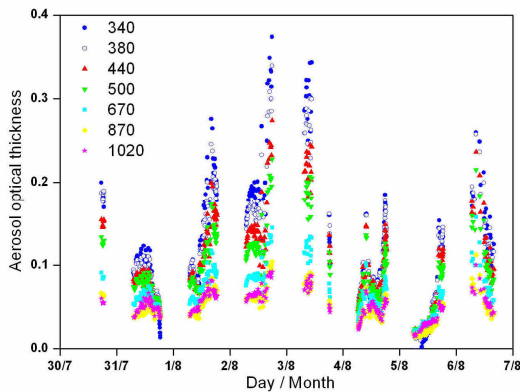


Figure 3. Aerosol optical thickness evolution along the complete field campaign for the seven channels of the CIMEL CE318 sunphotometer.

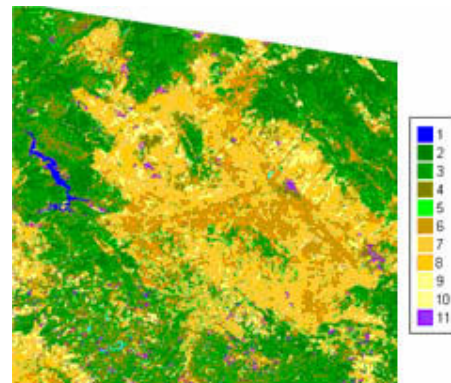
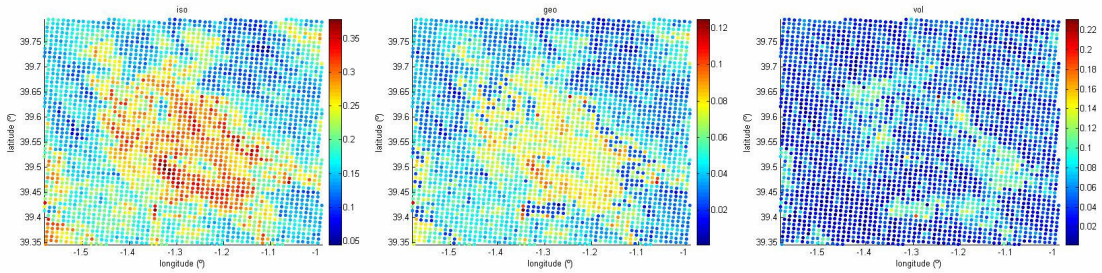


Figure 4. Land use Classification of the study area from Landsat 5 image: 1.water, 2. pine trees, 3. low density pine trees and shrubs, 4. shrubs, 5. irrigated crops, 6. vineyards, 7. low density vineyards, 8. very low density vineyards, 9. herbal crops, 10. bare soil, 11. urban areas.



**Figure 5: isometric, volumetric and geometric Kernels of the MOD43B1 product over the study area.**

### 1.4 Satellite data

For this study specifically programmed CERES observations in PAPS (Programmable Azimuth Plane Scanning Mode) mode have been used. Usually CERES operates in Cross-Track scanning sampling mode, looking at the surface in the orthogonal plane to its orbit, but it can be programmed to scan over a specific area changing azimuthally the observation plane. This special mode of operation provides a great number of radiances and fluxes over the same area from different observation and illumination angles. (Figure 6).

For *GERB* validation purposes we have used enhanced spatial resolution data (*GERB High Resolution*) (Figure 7), where the resolution of the computed fluxes is improved through the combination of well-calibrated *GERB* broadband data with SEVIRI narrow-band high-sampling-rate data. The resolution enhancement process transforms accurate fluxes computed at *GERB* footprint original resolution (nominally 50 km x 50 km at nadir) to a 3\*3 SEVIRI footprint resolution (nominally 9 km x 9 km at nadir) (Gonzalez et al)

Due to the reasonable homogeneity of the study area and the representativity of the VAS and mobile station measurements (Lopez et al, 2007) we can perform simulations over 4 *GERB* High resolution pixels for validation purposes.

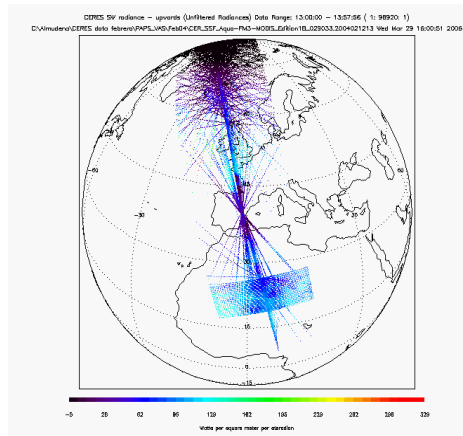


**Figure 6: Sample of CERES FM3 TOA Shortwave Radiances over the VAS. 12th February 2004, 13z**

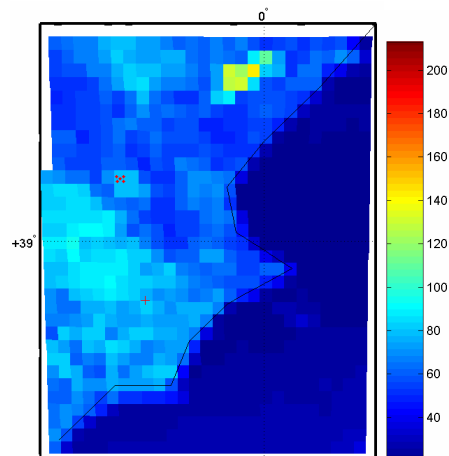


**Figure 7: Sample of GERB High Resolution SW radiances data, 31<sup>st</sup> of July 2006.**

### 1.5 Collocation algorithm:

*CERES* PAPS footprints vary in location and size from one to another. In order to know the BRDF at *CERES* scale it will be necessary to convolve the Imager Surface Properties with the *CERES* Footprint Point Spread Function. (Figure 8).

First, we determine the limits of every *CERES* footprint and then we locate the pixels from MODIS kernels that are within every *CERES* footprint. (Figures 9 and 10).

The collocation algorithm must be able to handle the shape of the *CERES* footprints in PAPS mode and also take into account the scanning direction because of the asymmetry of the *CERES* PSF

The results are the weighted means where the weighting corresponds to the PSF.

$$\bar{x} = \frac{\int_{FOV} P(\delta, \beta) \cdot x(\delta, \beta) \cos \delta \cdot d\beta \cdot d\delta}{\int_{FOV} P(\delta, \beta) \cdot \cos \delta \cdot d\beta \cdot d\delta}$$

With respect to GERB analysis, the type of data selected is independent of the PSF of the instrument, being just necessary to consider the dimensions of the footprints and average the kernels over them to obtain the pixels BRDFs.

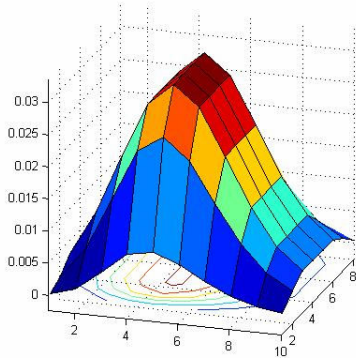


**Figure 8: CERES Point Spread Function**

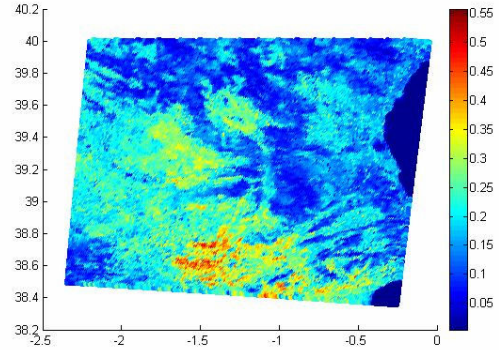


**Figure 9: Sample of one of the MOD43 product kernels (in this case isometric) used in the collocation algorithm to build the BRDF**

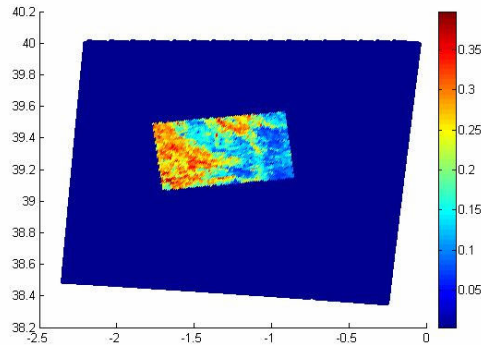


**Figure 10: Sample of the application of the collocation algorithm to extract the MODIS kernel pixels within the CERES footprint**

## 2. RESULTS

We have carried out two radiance and fluxes simulations for every CERES and GERB footprint, one for the shortwave range and another for the longwave. In the case of CERES it has been necessary to develop a collocation algorithm to calculate a specific BRDF for each CERES footprint. For GERB, the fixed situation of the pixels reduces the complexity of the problem.

### 2.1 CERES comparisons

A sampling of the results of the radiative transfer simulations for CERES is shown in Figures 11 and 13. From the graphs we can infer that radiances in the shortwave present high anisotropy between forward and backward scattering directions (figure 12). All cases analysed show that radiances in the backward scattering direction under clear sky conditions are higher than in the forward ones. TOA Flux

simulations have been performed at a reference level of 20 km, level that has been determined as the optimal reference level for defining TOA fluxes in Earth Radiation Budget studies. The definition of this effective level simplifies the comparisons with plane-parallel modelled fluxes, since, at this level, it is not necessary to consider horizontal transmission of solar radiation through the atmosphere (Loeb et al, 2002).

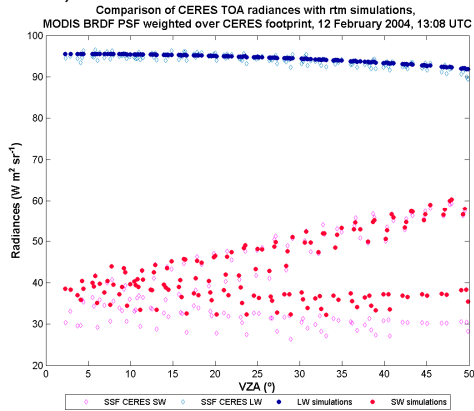


**Figure 11 : TOA radiances comparison for Aqua FM3, 12th February 2004**

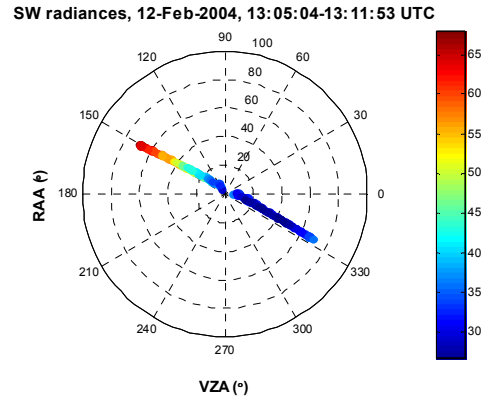


**Figure 12: CERES TOA SW radiances and geometry. Radial axis corresponds to VZA and azimuthal direction corresponds to RAA**

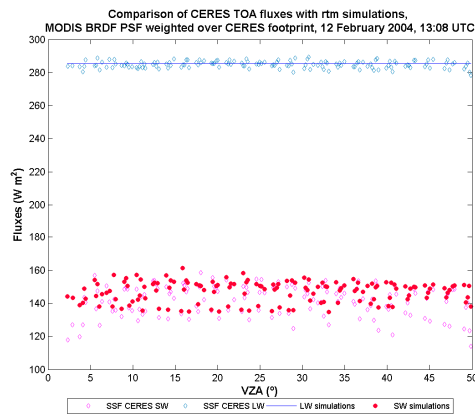


**Figure 13: TOA fluxes comparison for Aqua FM3, 12th February 2004**

As it can be seen in the plots, the agreement between satellite data and simulations is really good for radiances and fluxes comparisons both in shortwave and longwave. It is significant that the methodology is able to reproduce the anisotropic behavior of the shortwave radiances, showing low RMSE in the comparisons (Table 1).

## 2.2 GERB comparisons

As regards GERB comparisons, we have run simulations every 15 min, from 7:00 until 17:00 UTC, for the 1<sup>st</sup> of August 2006 over the 4 selected footprints that cover the study area. As it can be seen in the plots, the comparisons between simulated and measured radiances and fluxes show good agreement, as well as in the CERES case. RMSE in SW radiances are of the same order as the obtained for CERES comparisons. In relation to the derived fluxes, GERB shows higher RMSE than CERES in the comparisons, needing this problem further investigations (Table 1).



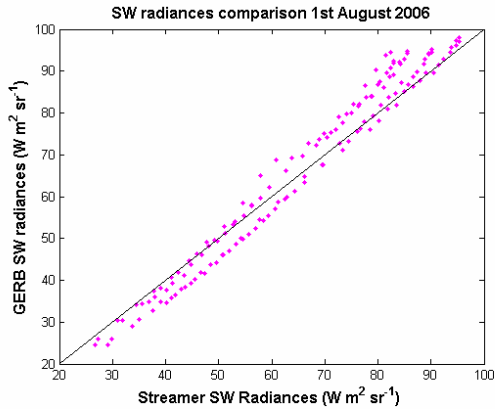


Figure 14: TOA SW radiances comparison for GERB High Resolution Data, 1<sup>st</sup> August 2006

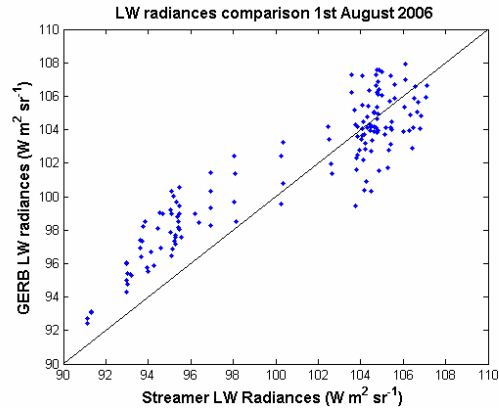


Figure 15: TOA LW radiances comparison for GERB High Resolution Data, 1<sup>st</sup> August 2006

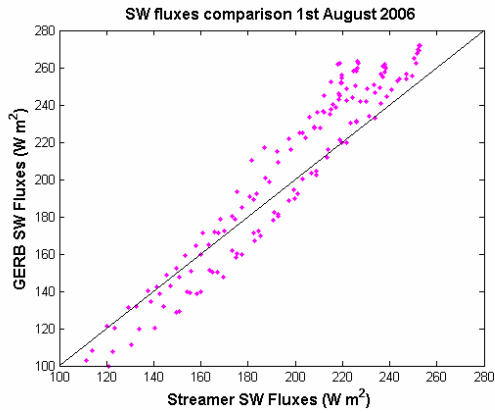


Figure 16: TOA SW fluxes comparison for GERB High Resolution Data, 1<sup>st</sup> August 2006

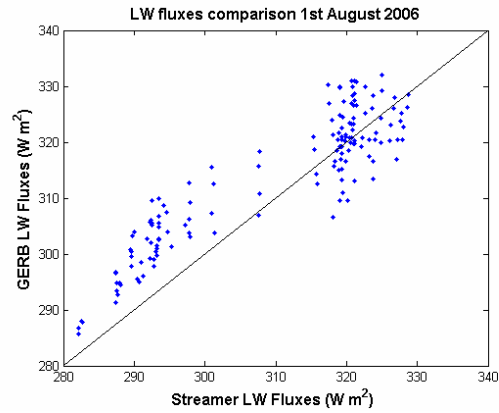


Figure 17: TOA LW fluxes comparison for GERB High Resolution Data, 1<sup>st</sup> August 2006

SENSOR and date	RMSE for SW radiances ( $W m^{-2} sr^{-1}$ )	RMSE for LW radiances ( $W m^{-2} sr^{-1}$ )	RMSE for SW fluxes ( $W m^{-2}$ )	RMSE for LW fluxes ( $W m^{-2}$ )
CERES SSF FM2 12 <sup>th</sup> Feb 2004	4.1	0.8	8.6	2.2
GERB High Resolution 1 <sup>st</sup> August 2006	4.3	2.3	17.5	7.1

Table 1: Root Mean Square Errors of the comparisons

### 3. CONCLUSIONS

The methodology here shown is able to reproduce *CERES* and *GERB* TOA unfiltered radiances and fluxes under clear sky conditions showing low RMSEs. Simulated radiances finely reproduce the anisotropy of the radiance field at the TOA, being forward and backward features of TOA SW radiances well reflected in the results. The inclusion of a higher resolution BRDF in the methodology has significantly improved the comparison between simulated and measured fluxes and the global nature of the MODIS BRDF satellite data will allow further studies over wider areas (Velazquez et al, 2006).

*CERES* dedicated PAPS observations over the VAS are of great value to develop the methodology to

validate low spatial resolution remote sensing data and products because of the large amount of angular information they provide. In this way, the methodology has been first assessed for CERES and then applied to *GERB* products. The comparison between simulations and *CERES* well calibrated and validated data provides a good indicator of the reliability of the methodology to be applied as a validation tool for *GERB*.

#### 4. REFERENCES

Gonzalez L., A. Hermans, S. Dewitte, A. Ipe, G. Sadowski, N. Clerbaux. Resolution Enhancement of GERB data, RMIB Technical Note: MSG-RMIB-GE-TN-0003

Key, J. and A. J. Schweiger (1998): Tools for atmospheric radiative transfer: Streamer and FluxNet, *Computers & Geosciences*, **24**(5), 443-451.

Loeb, N.G, S. Kato and B.A.Wielicki. Defining Top-of-Atmosphere Flux Reference Level for Earth Radiation Budget Studies. *Journal of Climate*, vol: 15, n°22, pp3301-3309.

Lopez-Baeza, E., A. Velazquez, and the SCALES PROJECT TEAM (2004): Towards a methodology for the validation of low spatial resolution remote sensing data and products. The Valencia Anchor Station. Committee on Space Research (COSPAR). 35th COSPAR Scientific Assembly. Scientific Commission A: Space Studies of the Earth's Surface, Meteorology and Climate. Biological and Physical Processes on Land. Paris, France, 18 – 25 July 2004

Lopez-Baeza, E., S. Vidal, A. Cano, C. Domenech, A. Geraldo Ferreira, C. Millan-Scheiding, C. Narbon, J. Sanchis, A. Velazquez. (2007) Representativity of the Valencia and the Alacant Anchor Stations in the context of validation of remote sensing algorithms and low-resolution products. Proceedings of the Joint 2007 EUMETSAT/AMS Conference

Stamnes, K., S.C. Tsay, Wiscombe and I. Laszlo, (2000): A general-purpose, numerically stable computer code for Discrete-Ordinate\_method Radiative Transfer in Scattering and Emitting Layered Media, DISORT Report v1.1.

Velazquez, A. E. Lopez-Baeza, , G.L Smith, Z. P. Szewczyk (2004). CERES Operations for the Valencia Anchor Station in Support of GERB Validation Efforts. CERES SCALES Campaigns. Proceedings of the 13th Conference on Satellite Meteorology and Oceanography

Velazquez, A. S. Alonso, A. Bodas-Salcedo, S. Dewitte, C. Domenech, J. Gimeno, J.E. Harries, J. Jorge Sanchez, A. Labajo, N. G. Loeb, D. Pino, A. Sanchis, G.L. Smith, Z. Peter Szewczyk, R. Tarruella, J. Torrobella, E. Lopez-Baeza (2005). Comparison of top of the atmosphere GERB measured radiances with independent radiative transfer simulations obtained at the Valencia Anchor Station area. Remote Sensing of Clouds and the Atmosphere X. Proc of SPIE 5979

Velazquez, A., S. Alonso, C. Doménech, J. Gimeno, J. Jorge Sanchez, A. Labajo, N. G. Loeb, D. Pino, T., Rius, A. D. Sanchis, G. L. Smith, Z. P. Szewczyk, R. Tarruella, J. Torrobella y E. López-Baeza (2006) Use of CERES PAPS observations over the Valencia Anchor Station to validate low spatial resolution remote sensing data and products. Proceedings of the 12th Conference on Atmospheric Radiation

Wanner, W, X.Li, and A.H. Strahler (1995): On the derivation of kernels for kernel-driven models of bidirectional reflectance, *J. Geophys. Res.*, **100**, pp. 21077-21090

Wilber, A.C., D.P. Kratz, and S.K. Gupta (1999): Surface Emissivity Maps for Use in Satellite Retrievals of Longwave Radiation. NASA/TP-1999-209362